Modular Analysis of Tropical-Cyclone Structure

Francis Fendell and Gregory Smetana

Northrop Grumman Aerospace Systems, Redondo Beach, CA 90278, USA

Paritosh Mokhasi

Wolfram Research, Inc., Champaign, IL 61820, USA

(Dated: December 16, 2015)

Abstract

In the early 1970s, George Carrier and coworkers undertook a modular approach to modelling the internal thermofluid-dynamics of tropical cyclones of tropical-depression-or-greater intensity. A novel, relatively simplistic, approximate analysis of the vortex, idealized as axisymmetric, was carried out in the asymptotic limit of large Reynolds number, so that inviscid and diffusive subdomains of the structure were distinguished. Little subsequent work has followed this line of investigation. The indifference has proven problematic because accurate prediction of tropical-cyclone intensity remains a challenge for operational forecasting, despite decades of effort at direct integration of comprehensive boundary/initial-value formulations. A contributing factor is that, to achieve solution in real time, such computational treatment of the entire vortex invariably resorts to coarse gridding, and key features remain inadequately resolved. Accordingly, here the modular approach is revisited, with the assistance of: recent observational insights; greatly enhanced computer-processing power; and convenient computational software, which facilitates implementation of a semi-analytic, semi-numerical methodology.

Nomenclature

Variables

Symbol	Description	Units
RH	relative humidity	-
ρ	density	$\mathrm{kg\,m^{-3}}$
p	pressure	Pa
S	entropy	$\mathrm{m^2\,s^{-2}\,K^{-1}}$
T	temperature	K
Y	water vapor mass fraction	-
z	altitude	m

Constants

Symbol	Description	Value	Units
σ	ratio, molecular weights of water vapor and air	0.622	-
c_p	specific heat capacity, const p	10^3	$\mathrm{m^2\,s^{-2}\,K^{-1}}$
g	gravity	9.81	$\mathrm{m\,s^{-2}}$
L	specific latent heat, phase transition for water substance	2.5×10^6	$\mathrm{m^2\,s^{-2}}$
R	gas constant for air	287.1	$\mathrm{m^2\,s^{-2}\,K^{-1}}$

Subscripts

Symbol	Description
amb	ambient
eye	eye
min	closest approach within the bulk-vortex module to the axis of rotation
moist	moist adiabat

s	ocean-surface value; saturated (in core module)
sat	saturated
switch	lifting condensation level
trop	tropopause
underrun	eye-underrunning moist (usually saturated) air
v	water vapor
vsat	saturated water vapor

Superscripts

Symbol	**Description**
$'$	dimensional quantity; normalized mass fraction

Contents

I. BOUNDING TROPICAL-CYCLONE INTENSITY

Although it provides no insight into size, lifespan, precipitation, storm surge, or tornadogenesis, traditionally the one parameter taken to characterize best the intensity of a tropical cyclone is the peak sustained low-level wind speed within the vortex. Formally, NOAA takes this to be the maximal one-minute-averaged swirl speed at 10-m altitude above the air/sea interface, at any lateral distance from the center. Other meteorological agencies around the globe adopt three-minute or ten-minute averaging, and typically arrive at a lower value. (In many contexts, the tropical cyclone will continue to be characterized by the highest value achieved during its lifespan, even if the system since has declined to lower peak speed.) Also, the air/sea interface can become so convoluted and/or ill-defined under high wind shear that sometimes the peak sustained wind speed holding at an altitude as high as a kilometer above the nominal air/sea-interface height is adopted. In any case, although definitive values are given for the intensity of a tropical cyclone, in fact, comprehensive measurement is almost never available. In the Atlantic basin, and sometimes in the eastern North Pacific, the values often are best estimates inferred from measurements made by reconnaissance aircraft flying a few transects (legs) of the vortex at altitude of about 3 km, at intermittent intervals of time. Elsewhere in the tropics, the values for intensity are estimates from subjective interpretation of cloud imagery taken from satellites (i.e., from pattern recognition, the so-called Dvorak

method). In general, any cited intensity is uncertain to within 5-10% at least.

Accordingly, of interest is the peak swirl theoretically achievable in a given spawning ambient atmosphere, upon postulation of the physical processes occurring within the system. Here we idealize the system as a steady, axisymmetric vortex contained within a conceptual, uniformly rotating (at the angular speed of the locally normal component of the Earth's rotation), right circular cylinder with an open lateral boundary. The cylinder has an impervious slippery isobaric isothermal horizontal lid at the altitude of the tropopause (to be defined), and an impervious no-slip nonisobaric horizontal bottom at the altitude of the nominal air-sea interface. Implicitly, there is a low-level inflow in the cylinder, ascent in the core near the axis of rotation (and symmetry), and upper-level outflow from the cylinder. However, we in this section deal minimally with the secondary (radial/axial) flow, and derive thermo-hydrostatically and cyclostrophically based bounds on the swirl speed achievable in the cylinder. We focus on sensible-heat-and-moisture content of the throughput entering the cylinder at the periphery, for a once-through transit and discharge back to the surrounding atmosphere. The intake is regarded as convectively unstably stratified, and the discharge is likely to be stably stratified.

Thus a vortex of at least tropical-depression intensity is taken to exist in the cylinder. The ambient is somewhat modified from the mean autumnal maritime-tropical sounding (e.g., Jordan ambient) because on a typical day there is no tropical cyclone present. The diffusive transfer from sea to air of heat and moisture across the bottom boundary of the cylinder is at about ambient level, and is not significantly enhanced above ambient level. The heat and moisture already present in the atmospheric intake are shown to be readily sufficient to sustain the vortex without the need for any hypothesized augmented transfer of enthalpy from the underlying ocean.

We take the adopted ambient stratification to hold at all altitudes at the periphery, even though the upper-tropospheric efflux disrupts that ambient stratification at higher altitudes in the troposphere.

Our goal is to compute the lateral pressure deficit from ambient, holding at sea level under various vertical columns of air within the vortex. For a hydrostatic approximation, the sea-level pressure is the weight per cross-sectional area of a vertical column of fluid. Thus, the sea-level pressure anomaly is an integral over altitude of the discrepancy of the local density

from ambient density. If the top of the vortex is an isobaric isothermal lid, then any sea-level-pressure anomaly is owing to processes within the vortex. In particular, sea-level air rising on a moist-adiabatic locus of thermodynamic states in the idealized eyewall of a hurricane (or in the core of a well-developed tropical storm) can generate a sea-level pressure anomaly of no more than a few tens of hectoPascals (hPa, equivalent to millibars). Condensational heating, to counteract expansional cooling during ascent to lower pressure, can effect no greater density reduction. Under a cyclostrophic approximation to the conservation of radial momentum (suitable for the axisymmetric right-circular-cylinder geometry), with the radial profile of the swirl component of relative velocity being of Rankine-vortex form, and with the density being held approximately constant with radius, then the peak swirl speed cannot exceed about 40 m/s. This approximates the peak speed of a strong tropical storm and is substantially smaller than the speed recorded in the highest category of hurricane.

To achieve the columnar reduction of density that results in a sea-level-pressure anomaly of nearly 100 hPa or even greater, an anomaly that has been observed in exceptional incidents, some other physical process must be involved. That process is compressional heating of relatively dry, tropopause-level air, during descent seaward to higher pressure in a central eye. The pressure deficit so achievable is far more than the magnitude that is consistent with the nearly 100 m/s peak swirl speed observed in the very intense hurricanes. In practice, the eye is not entirely dry, owing to evaporative cooling related to the influx to the eye of condensate generated in the adjacent eyewall. Also, the eye may not extend the entire distance from the tropopause seaward to ocean surface; some inflowing moist (possibly saturated) air may underrun a partially inserted, central eye.

An inconsistency in the foregoing discussion is that the computation of the lateral pressure differences is at sea-level altitude. However, the swirl-speed conversion utilizes a cyclostrophic balance. A diffusion-free approximation to the conservation of radial momentum holds in the inviscid flow above the roughly one-kilometer-thickness, ocean-surface-contiguous boundary layer. Nevertheless, the adopted procedures seem a reasonable way to proceed.

The analysis that follows provides quantitative details in support of the foregoing discussion. Even so, the analysis leaves many notable details unresolved. Why do (statistically) only about half of tropical storms develop eyes, and can we anticipate which tropical storms will evolve to become hurricanes? Why do (statistically) only about one-third to one-half of

hurricanes generate well-defined eyes (i.e., become major hurricanes), and can we anticipate which hurricanes will? These transitions may depend on changes in ambient conditions, but plausibly, once a tropical system achieves the levels of intensity under discussion, the transitions may depend primarily on thermo-fluid-dynamics internal to the vortex. Also, the high peak swirling of a hurricane is observed near the base of the eyewall; the wind in the eye is famously calm. Hence, with increasing height, the eye/eyewall interface must slope radially outward, away from the central vertical axis, so that the density reduction in the eye may be cited plausibly as the physical mechanism supporting enhanced swirling in the lower eyewall through enhanced sea-level pressure deficit. The entrainment/detrainment between the eye and the eyewall in a steady model remains to be explored.

II. EQUATIONS

A. Ambient Profiles with Altitude

(calculated from $T_{amb}[p]$, $\mathrm{RH}_{amb}[p]$, taken as available from sounding)

- Equations of State

$$p = \rho R T \tag{1}$$

$$\sigma p_v = \rho_v R T \tag{2}$$

- Definition of Water Vapor Mass Fraction

$$Y = \rho_v / \rho \tag{3}$$

Whence,

$$Y = \sigma \, \mathrm{RH} \, P(T)/p \tag{4}$$

- Definition of relative humidity

$$\mathrm{RH} = p_v / P(T) \tag{5}$$

- Hydrostatics

$$\frac{\partial p}{\partial z} = -\rho g \tag{6}$$

B. Moist Adiabat Profiles

Since Y is taken constant on a dry adiabat,

$$\left(\frac{T}{T_{ref}}\right)^{\frac{\gamma}{\gamma-1}} = \frac{p}{p_{ref}} = \frac{p_v}{(p_v)_{ref}} \tag{7}$$

where $\gamma/(\gamma-1) = R/c_p$.

Let $(T_{sat})_{onset}$ be the lifting-condensation-level temperature and $T_{ref} \equiv (T_{amb})_s$ be the sea-level-ambient temperature, so (for $\gamma = 1.4$)

$$\left(\frac{(T_{sat})_{onset}}{(T_{amb})_s}\right)^{3.5} = \frac{P[(T_{sat})_{onset}]}{[\,\mathrm{RH}\,]_{amb}]_s P[(T_{amb})_s]} \tag{8}$$

This gives the temperature at which surface air in the ambient would saturate if lifted dry adiabatically. The temperature implies a pressure on the adiabat.

Once saturated, the moist adiabat follows the following locus of thermodynamic states, to rough approximation (the condensate is taken to fall out, but the air retains the heat of phase change):

$$c_p dT + L\sigma d\{P[T]/p\} - \frac{dp}{\rho} = 0 \tag{9}$$

where $T(p_{onset}) = (T_{sat})_{onset}$.

The state for which this $T(p)$ curve crosses the $T_{amb}(p)$ curve is identified as the tropopause. The height of the tropopause is identified from $z_{amb}(p)$, inverse of $p_{amb}(z)$.

Note: The moist-adiabat locus here is based on the total energy $c_pT + LY + gz + q^2/2 = const$, where $q^2/2$ (kinetic energy) is about a 1.5% contribution or less, and is discarded for present purposes.

Integrate from the tropopause seaward to find the thermodynamic state holding at the base $z = 0$:

$$\frac{dp}{dz} = -\rho g \tag{10}$$

$$c_p \frac{dT}{dz} + \sigma L \frac{d}{dz}[P(T)/p] - \frac{1}{\rho}\frac{dp}{dz} = 0 \tag{11}$$

$$p(z_{trop}) = p_{trop} \tag{12}$$

$$T(z_{trop}) = T_{trop} \tag{13}$$

Remember to drop the terms with L thenceforth if T increases in value to $(T_{sat})_{onset}$ before $z = 0$ is reached; i.e., switch over to the dry adiabat below the lifting condensation level. Note the value of $p(z = 0)$; this is henceforth cited as $p_{moist}(z = 0)$, or $p_{moist,s}$.

There is a self-consistency issue that may call for iteration of the moist-adiabat result. The ambient-sea-level state has been adopted as the reference state for the adiabat, but is really not pertinent to a vertical column in the core. The final state computed at $z = 0$ should be adopted as the reference state for: a recalculation of temperature vs pressure; re-identification of the tropopause; and reassignment of altitude. Presumably, this iterative process quickly converges, so an initial estimate of the sea-level state is recovered as the updated sea-level state, to satisfactory approximation.

C. Eye Adiabat Profiles

Integrate seaward from the tropopause for an unsaturated eye. Thus

$$\frac{dp}{dz} = -\rho g \tag{14}$$

$$c_p \frac{dT}{dz} + \sigma L \,\mathrm{RH}\, \frac{d}{dz}[P(T)/p] - \frac{1}{\rho}\frac{dp}{dz} = 0 \tag{15}$$

$$p(z_{trop}) = p_{trop} \tag{16}$$

$$T(z_{trop}) = T_{trop} \tag{17}$$

The key new parameter here is RH, which denotes the relative humidity in the eye. If $RH = 0$, the eye is totally dry, and, for this extreme idealization, the pressure at sea level is quite decremented from $p_{amb,s}$, the sea-level ambient value (given).

We envision some evaporative cooling because condensate (ice crystals and droplets) fall into the eye and are evaporated. The value of RH could vary with altitude, but the simplest

procedure is to hold it constant with height, at some value between 0 and 1. At $RH = 1$, all the heating in the eyewall owing to condensation is reversed in the eye owing to evaporation.

In the current notebook, there is an attempt to deal with a moist (in fact, saturated) inflow underrunning an eye that descends only part of the distance from the tropopause to the sea surface. So for $z_{underrun} < z < z_{tropopause}$, with $z_{underrun}$ specified (if $z_{underrun} = 0$, there is no underrun), or for $p_{tropopause} < p < p_{underrun}$, with $p_{underrun}$ specified [if $p_{underrun} > (p_{moist})_{surface}$, there is no underrun], use the above equations in the eye. In the underrun, use the same equations except $RH = 1$. However, at $z = z_{underrun}$, (or $p = p_{underrun}$ – a value for one implies a value for the other), there is a contact surface: pressure p is continuous, but density ρ and temperature T are discontinuous. Also, the total energy is continuous (within our approximation that the kinetic energy is negligible). So

$$c_p T_+ + \sigma L(RH) P(T_+)/p_{underrun} = c_p T_- + \sigma L P(T_-)/p_{underrun} \tag{18}$$

where

$T_+ = T(z_{underrun+})$, known

$T_- = T(z_{underrun-})$, to be found

and, for completeness, if $\rho_- = \rho(z_{underrun-})$,

$\rho_- = p_{underrun}/(RT_-)$

Then one integrates moist-adiabat equations

$$\frac{dp}{dz} = -\rho g \tag{19}$$

$$c_p \frac{dT}{dz} + \sigma L \frac{d[P(T)/p]}{dz} - \frac{1}{\rho}\frac{dp}{dz} = 0 \tag{20}$$

to $z = 0$ to find the pressure at the surface beneath a partially inserted eye. Incidentally, note that the radially outward slope of the mean eye/eyewall allows hydrometeors in transient, vertically ascending cumulonimbi of the inner portions of the eyewall to penetrate into the eye, for subsequent evaporation.

D. Translation of Sea-Level Pressure Anomalies to Peak Swirl

Let swirl

$$v(r) = \begin{cases} V_{max}(r/r_{max}), & 0 < r < r_{max} \\ V_{max}(r_{max}/r), & r_{max} < r < \infty \end{cases} \tag{21}$$

This patching of a rigidly rotating core to a potential vortex (Rankine vortex) lets V_{max} be estimated from a cyclostropic balance by substitution and integration

$$\frac{v^2}{r} = \frac{1}{\rho}\frac{\partial p}{\partial r}, \qquad 0 \leq r \leq \infty \tag{22}$$

provided we estimate the density ρ (e.g., ascribe ρ some average value). Note that (22) does not furnish a local relationship between v and p, but between v and $\partial p/\partial r$.

For a tropical storm (no eye, so the moist adiabat holds near $r = 0$)

$$V_{max} = \left\{ \frac{2(p_{amb,s} - p_{moist,s})}{\rho_{amb,s} + \rho_{moist,s}} \right\}^{1/2} \tag{23}$$

For a hurricane with a partially inserted eye,

$$V_{max} = \left\{ \frac{2(p_{amb,s} - p_{eye,s})}{\rho_{amb,s} + \rho_{eye,s}} \right\}^{1/2} \tag{24}$$

For a hurricane with a fully inserted, non-rotating eye, it may be argued that there is no rigidly rotating core, so

$$V_{max} = \left\{ \frac{4(p_{amb,s} - p_{eye,s})}{\rho_{amb,s} + \rho_{eye,s}} \right\}^{1/2} \tag{25}$$

Conceptually, the peak swirl probably holds at low altitudes near the outer "boundary" of a rigidly rotating core, so the estimate in (25) is questionable. However, that suggestion remains to be supported, so at this point, there is little constraint regarding the lateral location of the peak swirl. For now, more pressure deficit arises for a fully inserted eye, and half of the pressure deficit might not need to be expended maintaining a rigidly rotating core. In any case, the absence of r_{max} in the expressions for V_{max} is noteworthy (and convenient).

Plots of total static energy (ignoring kinetic energy)

$$H(z) = c_p T(z) + L\frac{\sigma(RH)P(T(z))}{p(z)} + gz \tag{26}$$

for the various columns in the vortex are informative.

III. BOUNDARY LAYER DYNAMICS AND ENERGETICS

A. Dynamics (unchanged from a JFM paper for a constant-density model)

We first pursue solution for the boundary-layer flow over the large radial expanse from periphery to separation (wherever that occurs) because the dynamics in the boundary-layer module constrains the secondary flow in the bulk vortex. The steady axisymmetric flow is approximated as incompressible since the maximum speed achieved in a tropical cyclone rarely exceeds 100 m/s, so the Mach number rarely reaches even 0.3. The analysis is carried out in a non-inertial coordinate system rotating at the constant speed of that component of the rotation of the Earth which is normal to the local tangent plane. A simple down-gradient-diffusion model with a constant transfer coefficient, ascribed eddy-diffusion values, is examined, in the absence of observational evidence compelling the adoption of a more refined formulation. Other transfer models, however, are readily accommodated by the procedures developed below.

The conservation equations are

$$\nabla' \cdot \mathbf{q}' = 0 \tag{27}$$

$$\nabla'(q'^2/2) + (\nabla' \times \mathbf{q}') \times \mathbf{q}' + 2\mathbf{\Omega}'_{\mathbf{e}} \times \mathbf{q}' = -\nabla'\tilde{p}' - \nu'\nabla' \times (\nabla' \times \mathbf{q}') \tag{28}$$

where $\tilde{p}' = (p'/\rho'_{ref}) - (\mathbf{\Omega}'_{\mathbf{e}} \times \mathbf{r}')^2/2 + g'z'$, ρ'_{ref} denotes a reference density, the gravitational acceleration $\mathbf{g}' = g'\hat{\boldsymbol{z}}$, the velocity in inertial coordinates $\mathbf{v}' = \mathbf{\Omega}'_{\mathbf{e}} \times \mathbf{r}' + \mathbf{q}'$, the angular velocity of the earth is denoted $\mathbf{\Omega}'_{\mathbf{E}}$, the normal to the local tangent plane is denoted $\hat{\boldsymbol{z}}$, $\mathbf{\Omega}'_{\mathbf{e}} = \Omega'\hat{\boldsymbol{z}}$, $\Omega' = (\mathbf{\Omega}'_{\mathbf{E}} \cdot \hat{\boldsymbol{z}})$ and ν' denotes the kinematic eddy viscosity.

Non-dimensionalization is introduced by letting

$$\mathbf{q} = \mathbf{q}'/(\Psi'_o\Omega')^{1/2}, \qquad p = \tilde{p}'/(\Psi'_o\Omega'), \qquad \mathbf{r} = \mathbf{r}'/(\Psi'_o/\Omega')^{1/2} \qquad \text{and} \qquad E = \nu'/\Psi'_0 \tag{29}$$

where the Ekman number $E \ll 1$ for circumstances of interest, and Ψ'_0 has the dimensions of a circulation. If Ψ'_0 is ascribed the value of the maximum swirl speed times the radius at which the maximum occurs, non-dimensionalization would employ unknown outputs, rather than prescribed inputs. Thus, we set $\Psi'_0 = \Omega' r'^2_0$ where r'_0 denotes the radial extent of the cylindrical domain.

Thus,

$$\nabla \cdot \mathbf{q} = 0 \tag{30}$$

$$\nabla(q^2/2) + (\nabla \times \mathbf{q}) \times \mathbf{q} + 2\hat{\boldsymbol{z}} \times \mathbf{q} = -\nabla p - E\nabla \times (\nabla \times \mathbf{q}) \tag{31}$$

These non-dimensional equations are studied in axisymmetric cylindrical polar coordinates (it is convenient to reserve the symbol w)

$$\mathbf{q} = u\hat{\boldsymbol{r}} + v\hat{\boldsymbol{\theta}} + \tilde{w}\hat{\boldsymbol{z}}, \qquad \boldsymbol{r} = r\hat{\boldsymbol{r}} + z\hat{\boldsymbol{z}} \tag{32}$$

At the top edge of the boundary layer, the gradient-wind equation is adopted as a lowest-order approximation to the conservation of radial momentum:

$$\pi_r = 2V + V^2/r \tag{33}$$

where, in the bulk vortex, $p(r,z) \to \pi(r)$, and $v(r,z) \to V(r)$, at the top edge of the boundary layer. For consistency with the boundary-layer solution, it is anticipated that the axial velocity component in the bulk vortex $\tilde{w}(r,z) \to E^{1/2}W(r)$ at the top edge of the boundary layer. This modest magnitude, in conjunction with continuity, suggests that, near the top edge of the boundary layer, the nonlinear convective terms in the radial-momentum equation are small relative to the terms retained in (33), at least at smaller radius where higher swirl holds.

If $\tilde{\zeta} = z/E^{1/2}$ (which implies that the boundary layer is $\mathrm{O}(E^{1/2})$ in thickness relative to r_0'), and if in the boundary layer

$$u = u_b(r,\tilde{\zeta}) + ..., \quad v = v_b(r,\tilde{\zeta}) + ..., \quad \tilde{w} = E^{1/2}w_b(r,\tilde{\zeta}) + ..., \quad p = p_b(r,\tilde{\zeta}) + ... \tag{34}$$

then the axial component of the momentum-conservation equation (31) takes the conventional form $\partial p_b/\partial\tilde{\zeta} = 0$ and the pressure field in the boundary layer is found from (33) if $V(r)$ is known. If

$$\psi = rv_b, \quad \Psi = rV, \quad \phi = ru_b, \quad w = 2^{-1/2}w_b, \quad x = r^2, \quad \zeta = 2^{1/2}\tilde{\zeta} \tag{35}$$

then, in terms of dimensional quantities,

$$\phi = r'u'/(\Omega' r_0'^2), \quad \psi = r'v'/(\Omega' r_0'^2), \quad w = w'/(2\Omega'\nu')^{1/2}, \quad \zeta = z'/(\nu'/2\Omega')^{1/2}, \quad x = r'^2/r_0'^2 \tag{36}$$

the boundary-layer thickness being $\mathrm{O}(\nu'/\Omega')^{1/2}$. Introduction of (34) and (35) into (30) and (31) gives

$$\phi_x + w_\zeta = 0 \tag{37}$$

$$\phi\phi_x + w\phi_\zeta + (\Psi^2 - \psi^2 - \phi^2)/2x - (\psi - \Psi) - \phi_{\zeta\zeta} = 0 \tag{38}$$

$$\phi\psi_x + w\psi_\zeta + \phi - \psi_{\zeta\zeta} = 0 \tag{39}$$

Patching to the bulk vortex gives, with $\Psi(x)$ taken as known and ζ_{edge} anticipated to be 'large',

$$\zeta \to \zeta_{edge} : \phi \to 0; \qquad \psi \to \Psi(x) \tag{40}$$

On $\zeta = 0$, no-slip conditions at a boundary impervious to convection are adopted:

$$\zeta = 0 : \phi = \psi = w = 0 \tag{41}$$

For the modest flow speeds holding in the vicinity of the periphery at $x = 1$, the nonlinear terms in (37)-(39) may be discarded as negligible relative to the linear terms. The solution to the linear balance of Coriolis 'force', pressure force, and friction, in which x enters parametrically only, was given by Ekman:

$$\phi \approx -[\Psi(x)]\sin(2^{-1/2}\zeta)\exp(-2^{-1/2}\zeta) \tag{42}$$

$$\psi \approx [\Psi(x)][1 - \cos(2^{-1/2}\zeta)\exp(-2^{-1/2}\zeta)] \tag{43}$$

$$w \approx 2^{-1/2}[\Psi_x(x)]\{1 - [\sin(2^{-1/2}\zeta) + \cos(2^{-1/2}\zeta)][\exp(-2^{-1/2}\zeta)]\} \tag{44}$$

Of particular interest is the boundary-layer exchange with the overlying vortex, $w(x, \zeta \to \zeta_{edge}) \equiv W(r)$ for $\Psi(x)$ of interest. For $x \to 1$, from (44)

$$w(x \to 1, \zeta \to \zeta_{edge}) \equiv W(x) \to 2^{-1/2}\Psi_x(x) \tag{45}$$

It is possible that (45) approximates adequately the exchange even for values of x sufficiently smaller than unity that (42)-(44) do not approximate adequately the solution to (37)-(41). We shall check this suggestion. In any case, dependence on the parameter ν' is displayed mainly in (36), since ν' does not appear in the boundary-value problem for $\phi, \psi, w, \Psi, \zeta$, and x, except implicitly in the quantity ζ_{edge}.

Since the absolute angular momentum is taken to be invariant along and across streamlines in module I, according to discussion given below, then, dimensionally, in the bulk vortex

$$r'v'(r') + \Omega' r'^2 = r'_0 v'_0 + \Omega' r'^2_0 \tag{46}$$

where $v'(r'_0)$, denoted v'_0, is regarded as known. Hence, under the non-dimensionalization discussed in (29) and thereafter, and in (34),

$$\Psi(r) = rV(r) = 1 + \varepsilon - x, \qquad \varepsilon \equiv v'_0/(\Omega' r'_0) \tag{47}$$

where $0 < \varepsilon \ll 1$ for parameter values of practical interest. Thus, ε, which may be characterized as a Rossby number, is significant near $x = 1$ only, and is not used to scale variables. Under (47), the circulation in the bulk-vortex module above the boundary layer is stable. There is downflow into the boundary layer as $x \to 1$. For values of $(2\Omega'\nu')^{1/2}$ of physical interest, the downflow is a very modest downdrift, according to (36).

However, accumulatively over x, the downdrift implicit in (45) and (47) implies a significant radial inflow ϕ within the boundary layer. Very little of this radial inflow stems from influx over ζ at $x = 1$, from (42) and (47) for $\varepsilon \to 0$. Moreover, as x decreases, the peak value Ψ of relative angular momentum ψ increases appreciably, in view of (40) and (47). Thus, on the left-hand sides of both (38) and (39), the nonlinear acceleration terms dominate the Coriolis term as x decreases. However, whereas, in the conservation of angular momentum equation (39), friction balances nonlinear advection across the entire boundary layer as x decreases, the presence of x in the denominator of some nonlinear terms suggests that an analytically convenient, purely inviscid balance well approximates the conservation of radial momentum equation (38) over the majority of the thickness of the boundary layer as x decreases:

$$\phi^2 + \psi^2 \approx \Phi^2 \tag{48}$$

Thus, at any fixed small value of x at which (47) and (48) hold, ψ monotonically decreases to zero, from a peak value near $(1 + \varepsilon)$, as ζ decreases, whereas ϕ monotonically increases from zero to a peak value approaching $(1+\varepsilon)$. Moreover, for small x, a two-layer substructure must develop because, in the immediate proximity of the sea surface $\zeta = 0$, the inflow ϕ must rapidly decrease from its peak value to zero within a relatively thin, swirl-free, frictional sublayer, to comply with the no-slip constraint (41). The evolution of the boundary-layer structure, from Ekman-layer profiles to a substantially different, two-layer, partially inviscid

character, has noteworthy implications for the boundary layer (and, as it turns out, for other modules of the tropical cyclone, especially the core). Selecting a uniformly suitable set of basis functions for a method-of-weighted-residuals integration of the boundary-value problem posed by (37) - (47) is challenging in view of this change of behaviour with x. Wherever (48) holds to good approximation, turbulent diffusion plays a diminished role, and the details of the eddy-diffusion coefficient are of reduced importance. The plausibility argument just given for (48) is supported by more quantitative argument (Carrier et al. 1994, Appendix B.2).

B. Energetics

Close examination of energetics-related properties of the tropical-cyclone boundary layer, when averaged over a time scale longer than any local convective process, has been often bypassed in the literature. In the context of accounting for boundary-layer effects on the entire vortex, generally focus has been on applying bulk-aerodynamic relations to quantify the transfer of sensible and latent heat at the sea-air interface. Such relations are formal, dimensionless statements of little utility until the embedded transfer coefficients are appropriately assigned; until then, the relations merely express one unknown in terms of another. While research continues, the often adopted and speculative extrapolation to high-wind-speed conditions of the wind-speed dependence holding for the transfer coefficients at relatively modest wind speed has been shown to be observationally invalid and to result in erroneous overestimates of sea-air transfer of enthalpy at high wind speed. It is disconcerting that intensity-related results obtained from many, if not most, tropical-cyclone models are very sensitive to the uncertain values assigned to parameters appearing in routinely adopted formulations of boundary conditions at the air-sea interface. Here, care is taken to incorporate the enthalpy transport into the boundary layer associated with downdrift from the overlying bulk-vortex module, as an important complement to roughly ambient-level sea-air transfer of enthalpy.

The point of view expressed in the last paragraph (that the majority of the heat-and-moisture content of the throughput being processed in the core of the vortex is already in the atmosphere of the autumnal maritime tropics, and greatly enhanced sea-to-air transfer of enthalpy under the high-speed portion of the vortex to enrich the throughput is neither necessary nor plausible) is distinctly a minority one. An alternative, far more commonly

adopted point of view is that proposed by Emanuel (2005):

> ... air flowing from high to low pressure would cool were no heat added to it... [H]eat flowing from sea into the air keeps it at nearly constant temperature. But there is a much more important source of heat: the enormous flow of energy that occurs when sea water evaporates into the inflowing air ... [E]vaporation ... effective in driving the storm occurs very near the hurricanes eyewall, where the winds are strongest. When hurricanes make landfall, they quickly die because they are cut off from their oceanic energy source.

In fact, isentropic thermodynamic relations are not pertinent to, and thus an inappropriate basis for anticipations about, properties of flow in frictional boundary layers; nearly saturated sea-level air can accept but little additional moisture; and hurricanes would die in two hours after landfall on even non-orographic coastlines were moment-to-moment enthalpy transfer crucial to their moment-to-moment maintenance, but hurricanes decay on (an inertial) time scale of 8-12 h after landfall.

Nevertheless, distractive controversies about sea-to-air enthalpy transfer persist because tropical cyclones involve an extreme environment, and the conditions are difficult to reproduce for corroboration of measurements. In situ observations of the core of the vortex remain particularly sparse, and those few readings available, even if possibly atypical (e.g., they are transient readings for a highly turbulent flow), are meticulously examined. Enhanced sea-to-air transfer of enthalpy under the eye of a tropical cyclone has been cited as the plausible source of high-entropy air reported near the sea surface in a small number of hurricanes. In any case, simple consideration of the relative lateral dimensions in a hurricane of the bulk vortex and of the base of the eye readily supports the findings of numerical models, namely, the practical significance for vortex intensity of any such local enhancement of sea-to-air transfer under the eye is nil.

For an incompressible model of the steady axisymmetric boundary-layer dynamics, the energetics is decoupled from the dynamics. Under the Reynolds analogy (so the turbulent Prandtl and Schmidt numbers are unity) and the hydrostatic approximation, Carrier et al. (1971) adopt the relation

$$u' \left(\frac{\partial E'}{\partial r'} \right) + w' \left(\frac{\partial E'}{\partial z'} \right) = \nu' \left(\frac{\partial^2 E'}{\partial z'^2} \right) \tag{49}$$

where, for a perfect gas with constant heat capacity c'_p over the range of temperatures of interest, the total stagnation energy E' is given by

$$E' \equiv c'_p T' + L' Y' + g' z' + q'^2/2 \tag{50}$$

Here, T' denotes temperature; L', the relevant latent heat of phase transition for water substance; and Y', the mass fraction (or, to the accuracy being pursued here, alternatively regarded as the mixing ratio) of water vapor. To be sure, Y' is inherently dimensionless, but we make this one exception in notation because we wish to emphasize the dependence on dimensional arguments. In (49), we have followed Carrier et al. (1971) in neglecting dissipation as a minor contributor to the total energy balance in a low-Mach-number, high-Reynolds-number flow. We depart from Carrier et al. (1971) in also ignoring radiative transfer because our steady model is being applied to a lower-atmospheric phenomenon of tropical-cyclone scale and of duration on the order of a week. For the boundary layer, observationally unsaturated virtually everywhere on a long-time average,

$$u' \left(\frac{\partial Y'}{\partial r'} \right) + w' \left(\frac{\partial Y'}{\partial z'} \right) = \nu' \left(\frac{\partial^2 Y'}{\partial z'^2} \right) \tag{51}$$

Although the boundary-layer-scaled coordinates have yet to be introduced, we have anticipated that the transversely diffusive terms dominate in (49) and (51). The convective coefficients $u'(r', z')$ and $w'(r', z')$ are available from the previously treated dynamics, so the transport equations (49) and (51) are linear parabolic convective-diffusive balances. Carrier et al. (1971, p. 160) characterize this formulation of the energetics as one in which '... the water vapor plays a important role in heat transfer only as a source of latent heat'.

For even a 100 m/s vortex, the contribution of the kinetic energy term $q'^2/2$ to the sum E' is uniformly $\leq O(1\%)$, and for many (though not all) purposes, $E' \rightarrow H' \equiv c'_p T' + L' Y' + g' z'$. Within the boundary layer, even a relatively thick boundary layer, the gravitational term is a small contributor to E' , $\leq O(3\%)$. Also, evaporation of spray would enhance the latent-heat contribution at the expense of the sensible-heat contribution in (50), and result in no net enhancement of E'. This net neutrality holds no matter how one contrives the droplet-size

distribution of the spray to facilitate fallout because any anomalous cooling of a lofted droplet is (?).

The boundary conditions are now addressed. At the nominal sea surface $z' = 0$, the temperature is taken constant at all radii at the known ambient level $T_{amb,s}$, any change (probably a noteworthy decrement owing to ocean mixing, especially under the core for larger, slower-translating vortices) being neglected. At the sea surface, the relative humidity $\mathrm{RH}'(r', 0)$ also is taken to be constant, at all radii, at the known ambient level $\mathrm{RH}_{amb,s}$, the value being fairly close to (but less than) unity. Since $z' = 0$ has been taken to be the datum for the gravitational potential, and in view of the no-slip approximation:

$$E'(r', 0) = c'_p T'_{amb,s} + L' Y'(r', 0), \quad E'_{amb,s} \equiv c'_p T'_{amb,s} + L' Y_{amb,s} \tag{52}$$

where, if $P'(T')$ denotes the saturation vapor pressure for water substance, exponentially dependent on temperature T',

$$Y'(r', 0) = \sigma\, \mathrm{RH}_{amb,s} P'(T'_{amb,s})/p'(r', 0), \qquad Y_{amb,s} \equiv \sigma\, \mathrm{RH}_{amb,s} P'(T'_{amb,s})/p'_{amb,s} \tag{53}$$

and σ denotes the ratio of the molecular weight of water vapor to that of dry air, ≈ 0.622

At the periphery of the domain $r' = r'_0$

$$E'(r'_0, z') \approx H'(r'_0, z') = c'_p T'_{amb}(z') + L' Y'_{amb}(z') + g' z' \tag{54}$$

$$Y'(r'_0, z') = Y'_{amb}(z') \tag{55}$$

where $T'_{amb}(0) = T'_{amb,s}$ and $Y'_{amb}(0) = Y'_{amb,s}$. More specifically, $T'_{amb}(z')$ and $\mathrm{RH}'_{amb}(z')$ are here typified by the Jordan mean sounding for the maritime autumnal tropical ambient in the western Atlantic. Although this observational ambient profile extends from nominal sea level to 500 hPa only, this suffices for current (though not all) purposes. Dunion and Marron emphasize that the distribution of individual soundings is bimodal, virtually all the individual soundings being convectively unstable but more moist or drier than the mean, and the mean itself being infrequently observed. We have followed Carrier et al. (1971) and many others in focusing on the Jordan mean sounding, but we note that the mean, while convenient, might not have special relevance for the stratification holding at the periphery of a tropical cyclone, more likely to pair in a moister ambient.

The following standard approximate relations seem adequate for our purposes for relating thermodynamic variables:

$$p'_a = \rho'_a R' T', \quad \sigma p'_v = \rho'_v R' T', \quad Y = \rho'_v / \rho'_a, \quad \gamma = c'_p / (c'_p - R') \tag{56}$$

$$\mathrm{RH}' = p'_v / P'(T'), \quad p' = p'_a + p'_v, \quad \rho' = \rho'_a + \rho'_v \tag{57}$$

$$p' - (1-\sigma) p'_{vap} = \rho' R' T' \quad \rightarrow \quad p' \approx \rho' R' T' \tag{58}$$

where subscript a denotes dry air, subscript v denotes water vapor, R denotes the gas constant for dry air, and γ denotes the ratio of specific heats for the mixture. The relations are inserted here because they enter into converting ambient sounding data from pressure coordinate p' to the axial spatial coordinate z'. In this connection, the hydrostatic relation suffices at the periphery $r' = r'_0$:

$$\frac{\partial p'}{\partial z'} = -\rho' g' \tag{59}$$

IV. DIFFUSIVE MODEL OF THE BULK-VORTEX MODULE

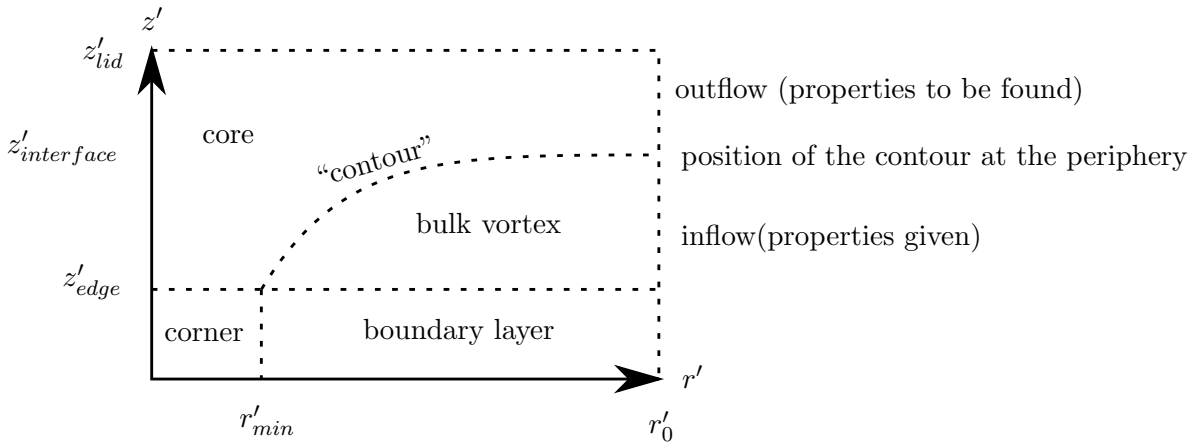

Notes:

- Prime superscript denotes a dimensional quantity.

- Parameters z'_{edge}, $z'_{interface}$, r'_{min}, r'_0 are given; the dimension z'_{lid} is computed in the (preliminary) tephigram method.

- The efflux (mass/time) at $r' = r'_0$, $z'_{interface} < z' < z'_{lid}$ equals the influx at $r' = r'_0$, $0 < z' < z'_{interface}$, in the steady state. Here, known ambient conditions hold only for $r' = r'_0$, $0 < z' < z'_{interface}$, where convectively unstable stratification holds for circumstances of interest.

- In the Carrier/Hammond/George treatment (CHG), the angular momentum per unit mass, $r'v'(r', z') + \Omega' r'^2$, is constant on streamlines (inviscid treatment). Here, v' is the (relative) swirl, i.e., swirl in non-inertial coordinates rotating with the Earth at the locally pertinent angular speed Ω', termed the Coriolis parameter. We also adopt $r'v'(r') + \Omega' r'^2 = r'_0 v'_0 + \Omega' r'^2_o$, where $v'(r'_o) = v'_0$, and $0 < \varepsilon \ll 1$ where $\varepsilon \equiv v'_0/(\Omega' r'_0)$, given.

- In the CHG treatment, in the bulk-vortex module,

$$Y(r', z') = Y_{amb}(z') \equiv Y(r'_0, z') \tag{60}$$

$$E'(r', z') = E'_{amb}(z') \equiv E'(r'_0, z') \tag{61}$$

where

$$\begin{aligned} Y &\equiv \rho'_v/\rho' = \sigma(RH)P'(T')/p' \\ E &= c'_p T' + L'Y + g'z' + q'^2/2 \\ &\approx c'_p T + L'Y + g'z' + v'^2/2 \end{aligned} \tag{62}$$

That is, the relative speed $q'^2 = u'^2 + v'^2 + w'^2 \approx v'^2$ in much of the vortex, and sometimes we drop even the v'^2 for tractability, as in the ambient $r' \to r'_0$. We cite the analysis in CHG for justification for the approximation in (60) and (61). Physically, CHG are saying that, as air in the bulk-vortex module moves to smaller r', on average, it is sinking slowly toward the boundary-layer module, for compatibility with the boundary-layer solution. As the air descends slowly to smaller z', the air takes on the

thermodynamic properties of air that formerly occupied that position at smaller z'. We recall from the tephigram method:

$$E'_{amb}(z') \equiv c'_p T_{amb}(z') + L' Y_{amb}(z') + g' z' + \cancelto{0}{\frac{v_0^2(z')}{2}} \tag{63}$$

$$Y_{amb}(z') \equiv \sigma R H_{amb}(z') P[T'_{amb}(z')]/p'_{amb}(z') \tag{64}$$

where, for a given ambient, we have the data

$$T'_{amb}(p'), RH_{amb}(p') \equiv p'_v(p')/P'[T'_{amb}(p')] \tag{65}$$

Also, we have [recall that $p'(r'_0, z') \equiv p'_{amb}(z')$]

$$\frac{dp'_{amb}(z')}{dz'} = -\rho'_{amb}(z') g' \tag{66}$$

$$\frac{dz'_{amb}(p')}{dp'} = -\frac{1}{\rho'_{amb}(p') g'} \tag{67}$$

In other words, we switch, whenever convenient, between the inverse functions $p'_{amb}(z') \leftrightarrow z'_{amb}(p')$. The reference state is taken to be $p'_{amb}(r'_0, 0) = p'_{ref}$, $T'_{amb}(r'_0, 0) = T'_{ref}$.

$$\sigma p'_v \equiv p'_v R' T' \tag{68}$$

$$p'(r', z') = \rho'(r', z') R' T'(r', z') \Rightarrow p'_{amb}(z') = \rho'_{amb}(z') R' T'_{amb}(z') \tag{69}$$

It will be convenient to approximate the equation of state for the gas as

$$p'(r', z') \approx \rho'_{amb}(z') R' T'(r', z') \tag{70}$$

in the bulk-gas module, for some purposes. This says merely that the density change in the bulk-vortex module is owing to hydrostatics mostly, because even the most intense hurricane is highly subsonic. We are also saying that we track water vapor only for its large condensational/evaporative heat; aside from that, water vapor is a trace species ($< 3\%$ by mass contribution to air).

- Since the flow is quasisteady and axisymmetric, the secondary flow is treated by the introduction of the streamfunction $\eta'(r', z')$; the radial velocity component $u'(r', z')$ and the axial velocity component $w'(r', z')$ are given by

$$\begin{aligned} \rho'(r', z')u'(r', z')r' &= -\frac{\partial \eta'}{\partial z'} \\ \rho'(r', z')w'(r', z')r' &= \frac{\partial \eta'}{\partial r'} \end{aligned} \tag{71}$$

If the aximuthial component of vorticity $\omega'_\theta = 0$ within the bulk-vortex module, then

$$\omega'_\theta(r', z') = -\left[\frac{\partial v'}{\partial r'} - \frac{\partial u'}{\partial z'}\right] = 0 \Rightarrow \frac{\partial}{\partial z'}\left(\frac{1}{\rho' r'}\frac{\partial \eta'}{\partial z'}\right) + \frac{\partial}{\partial r'}\left(\frac{1}{\rho' r'}\frac{\partial \eta'}{\partial r'}\right) = 0 \tag{72}$$

For a first cut, $\rho'(r', z') \to \rho'_{amb}(z')$ seems reasonable.

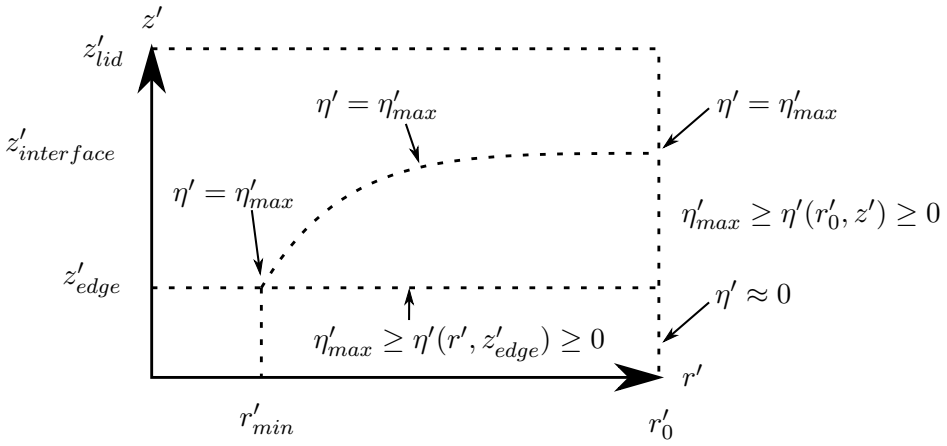

For a Dirichlet boundary condition on $\eta'(r', z')$ in the bulk-vortex module, at $r' = r'_0$, we adopt as an approximation,

$$\rho' u' r'_0 = -\frac{\partial \eta'}{\partial z'} \to \eta'(r'_0, z') - 0 = r'_0 \int_{z'_{edge}}^{z'} \rho'(r'_0, z')[-u(r'_0, z')]dz' \tag{73}$$

$$\eta'_{max} = r'_0 \int_{z'_{edge}}^{z'_{interface}} \rho'_{amb}(z')[-u'_{in}(z')]dz' \tag{74}$$

If $[-u'_{in}(z')] = -u'_{in}$, const, then

$$\eta'_{max} = \frac{r'_0}{g'} \left[p'_{amb}(z'_{interface}) - p'_{amb}(z'_{edge}) \right] (-u'_{in}) \tag{75}$$

The inflow u'_{in} follows, once η'_{max} is known.

- Aside:

$$\frac{\partial p'}{\partial r'}(r', z'_{edge}) \approx \rho'(r', z'_{edge}) \left[2\Omega' v'(r') + \frac{v'^2(r')}{r'} \right], \tag{76}$$

$$p'(r'_0, z'_{edge}) = p'_{amb}(z'_{edge}); v'(r') \text{ known:}$$

$$\begin{aligned} & r'v'(r') + \Omega' r'^2 = r'_0 v'(r'_0) + \Omega' r'^2_0 \\ & \rho'(r', z'_{edge}) = p'(r', z'_{edge}) / [R'T'(r', z'_{edge})] \\ & c'_p T'(r', z'_{edge}) + L'Y(z'_{edge}) + g' z'_{edge} + \frac{v'^2(r')}{2} = E'_{amb}(z'_{edge}) \end{aligned} \tag{77}$$

from (61). This yields a good approximation to $p'(r'_{min}, z'_{edge})$.

- Returning to estimation of $\eta'_{max} = \eta'(r'_{min}, z'_{edge})$:

$$\eta'(r', z_{edge}) - 0 = \int_{r'_0}^{r'} \underline{r}' \rho'(\underline{r}', z'_{edge}) w'(\underline{r}', z'_{edge}) d\underline{r}' \tag{78}$$

From boundary-layer (BL) dynamics,

$$\eta'_{max} = \int_{r'_{min}}^{r'_0} \underline{r}' \rho'(\underline{r}', z'_{edge}) \left[-w'_{BLedge}(\underline{r}') \right] d\underline{r}' \tag{79}$$

The entrainment into the boundary layer is estimated on an incompressible basis (constant-density treatment of the dynamics), but we accept this approximation. The density $\rho'(r', z'_{edge})$ is discussed just above. The quantity η'_{max} is an enormous number in SI units, and we use it for normalization of $\eta'(r', z')$ for computational convenience! So we deal with

$$\eta(r, z) = \eta'(r', z') / \eta'_{max} \tag{80}$$

where $r = r'/r'_0$, $z = z'/z'_{lid}$. We cannot readily non-dimensionalize z' against r'_0 because $r'_0 \gg z'_{lid}$. It is true that r'_{min} is closer to z'_{lid} in size, but we prefer not to use it for non-dimensionalization. We could use $[\nu'/(2\Omega')]^{1/2}$ for non-dimensionalizing z' in the bulk-vortex module, since $z'_{interface} \approx 3(z'_{edge})$ and $z'_{edge} \sim 5[\nu'/(2\Omega')]^{1/2}$. We did not so normalize when the bulk-vortex module was being treated as inviscid, but now only the dynamics (not the energetics) is inviscid in the bulk-vortex module.

- The pressure field in the bulk-vortex module is approximated by inviscid dynamics:

$$\begin{aligned} \frac{\partial p'}{\partial z'} &= -\rho' g' \\ \frac{\partial p'}{\partial r'} &= \rho' \left[2\Omega' v' + \frac{v'^2}{r'} \right] \\ p'(r'_0, z') &= p'_{amb}(z') \\ p'(r'_0, 0) &= p'_{ref} \end{aligned} \tag{81}$$

Conveniently, as a further approximation,

$$p'(r', z') - p'(r'_0, z'_{edge}) \doteq -g' \int_{z'_{edge}}^{z'} \rho'_{amb}(\underline{z}') d\underline{z}' - \int_{r'}^{r'_0} \rho'(\underline{r}', z'_{edge}) \left[2\Omega' v'(\underline{r}') + \frac{v'^2(\underline{r}')}{\underline{r}'} \right] d\underline{r}' \tag{82}$$

This approximation gives the pressure field to better accuracy along the top edge of the boundary layer and at the periphery, but less accurately elsewhere. Thus, the contour is given relatively accurately near its end "points" (r'_{min}, z'_{edge}) and $(r'_0, z'_{interface})$.

We review some in-hand results. In the above expression for $p'(r', z')$, $p'(r'_0, z'_{edge})$ is available from (66). Also, integration yields $p'(r', z'_{edge})$ from (76), and $T'(r', z'_{edge})$ is available from the expression $E'(r', z'_{edge}) = E'_{amb}(z_{edge})$ as given in the last of (77). Thus, $\rho'(r', z'_{edge}) = p'(r', z'_{edge})/[R'T'(r', z'_{edge})]$.

- Also,

$$\frac{S'(r', z')}{c'_p} = ln \left\{ \frac{\left[T'(r', z')/T'_{ref} \right]}{\left[p'(r', z')/p'_{ref} \right]^{\frac{\gamma - 1}{\gamma}}} \right\} \tag{83}$$

or

$$\frac{S'(r',z')}{R'} = ln\left\{\frac{\left[T'(r',z')/T'_{ref}\right]^{\frac{\gamma}{\gamma-1}}}{\left[p'(r',z')/p'_{ref}\right]}\right\} \tag{84}$$

- Accurate simple empirical expressions for L' are available in the notebook. Nominally, in thermodynamic equilibrium, freezing is at 273 K, but in fact in the atmosphere, freezing occurs closer to 263 or 253 K, owing to supercooling of condensate (as a consequence of scarcity of ice nuclei at temperatures near 273 K).

- Notice that a reconnaissance flight at 10 kft flies mostly in the core module if $z'_{interface} =$ 3 km.

V. SPECIFYING THE POSITION OF, AND PROPERTIES HOLDING ON, THE CONTOUR BETWEEN THE BULK-VORTEX MODULE AND CORE MODULE

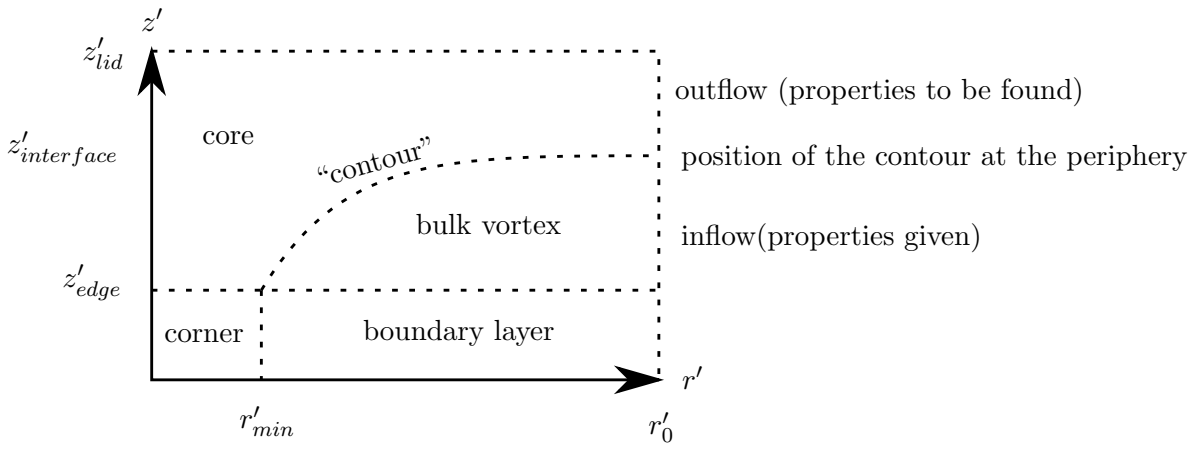

- We seek to define the "curve" ("contour") between (r'_{min}, z'_{edge}) and $(r'_0, z'_{interface})$, given the end "points".

- The contour position is defined by continuity of pressure $p'(r', z')$ because the dynamics on each side is inviscid. The swirl $v'(r', z')$ is continuous across the contour, but the radial

velocity component $u'(r', z')$ and axial velocity component $w'(r', z')$ are discontinuous, so the contour is a vortex sheet for the "secondary flow." The pressures $p'(r'_{min}, z'_{edge})$ and $p'(r'_0, z'_{interface})$ are known from the bulk-vortex analysis, with $p'(r'_{min}, z'_{edge}) > p'(r'_0, z'_{interface})$ in cases of interest.

- The temperature and density are discontinuous across the contour, which is a contact surface. The air is unsaturated in the bulk-vortex module, and saturated in the core module.

- The contour is a "streamline": there is no flow across it.

- The entropy, angular momentum, and total stagnation energy are constant on streamlines on the core side, which is taken to be inviscid. The value of each variable varies from streamline to streamline.

- Only the angular momentum is constant on streamlines on the bulk-vortex side, and for tractability, we examine only the special case for which the constant is invariant from streamline to streamline. Thus the model for the swirl in the bulk-vortex model is a potential vortex, generalized to the non-inertial coordinate system.

- We anticipate that the pressure $p'(r', z')$ on the contour decreases monotonically from $p'(r'_{min}, z'_{edge})$ to $p'(r'_0, z'_{interface})$, and that the curve $z'_{contour}(r')$ has monotonically decreasing but non-negative slope as one goes from (r'_{min}, z'_{edge}) to $(r'_0, z'_{interface})$. [The inverse representation $R'_{contour}(z')$ has a monotonically increasing and non-negative slope.] According to our model, r'_{min} decreases, but z'_{edge}, r'_0, and $z'_{interface}$ do not change, as the vortex intensifies, so the contour shape is not anticipated to be a sensitive indicator of intensity for a fixed ambient. The position r'_{min} is a sensitive indicator of intensity.

A. Bulk-Vortex Module

- Conservation of angular momentum

$$r'v'(r') + \Omega' r'^2 = r'_0 v'_0 + \Omega' r'^2_0 = \Omega' r'^2_0 (1 + \varepsilon) = \Gamma'_0 \tag{85}$$

- Pressure field

$$p'(r',z')-p'(r'_0,z'_{edge}) \doteq -g' \int_{z'_{edge}}^{z'} \rho'_{amb}(\underline{z}')d\underline{z}' - \int_{r'}^{r'_0} \rho'(\underline{r}',z'_{edge}) \left\{ 2\Omega' v'(\underline{r}') + \frac{v'^2(\underline{r}')}{\underline{r}'} \right\} d\underline{r}' \tag{86}$$

The two integrals in (86) can be tabulated ahead of time. Recall that $\rho'(r',z'_{edge})$ is obtained in the bulk-vortex-module equations. We much prefer this algebraic approximation for $p'(r',z')$ than to deal with a differential-equation/algebraic-equation mixture in defining the contour.

B. Core Side of Contour Streamline

$$r'v'(r') + \Omega' r'^2 = \Gamma'_0 \tag{87}$$

- 4 equations for the following 4 unknowns: $T'_{core}(r'_{min},z'_{edge})$, $T'_{core}(r'_0,z'_{interface})$, E'_{core}, S'_{core}

$$E'_{core}(r'_{min},z'_{edge}) \doteq c'_p T'_{core}(r'_{min},z'_{edge}) + \frac{L'\sigma P'[T'_{core}(r'_{min},z'_{edge})]}{p'(r'_{min},z'_{edge})} + g'z'_{edge} + \frac{v'^2(r'_{min})}{2} \tag{88}$$

$$E'_{core}(r'_{min},z'_{edge}) = E'_{core}(r'_0,z'_{interface}) = c'_p T'_{core}(r'_0,z'_{interface}) + \frac{L'\sigma P'[T'_{core}(r'_0,z'_{interface})]}{p'(r'_0,z'_{interface})} + g'z'_{interface} + \frac{v'^2(r'_0)}{2} \tag{89}$$

$$\frac{S'_{core}(r'_{min},z'_{edge})}{R'} = ln\left(\frac{T'_{core}(r'_{min},z'_{edge})}{T'_{ref}}\right)^{\frac{\gamma}{\gamma-1}} - ln\left(\frac{p'(r'_{min},z'_{edge})}{p'_{ref}}\right) + \frac{L'\sigma P'[T'_{core}(r'_{min},z'_{edge})]}{R'T'_{core}(r'_{min},z'_{edge})p'(r'_{min},z'_{edge})} \tag{90}$$

$$T'_{ref} = T'(r'_0, 0), \quad p'_{ref} = p'(r'_0, 0) \tag{91}$$

$$\frac{S'_{core}(r'_{min}, z'_{edge})}{R'} = \frac{S'_{core}(r'_0, z'_{interface})}{R'} = ln\left(\frac{T'_{core}(r'_0, z'_{interface})}{T'_{ref}}\right)^{\frac{\gamma}{\gamma-1}} - ln\left(\frac{p'(r'_0, z'_{interface})}{p'_{ref}}\right) + \frac{L'\sigma P'[T'_{core}(r'_0, z_{interface})]}{R'T'_{core}(r'_0, z'_{interface})p'(r'_0, z'_{interface})} \tag{92}$$

- Pressure field

$$E'_{core}(r'_{min}, z'_{edge}) = c'_p T'_{core}(r', z') + \frac{L'\sigma P'[T'_{core}(r', z')]}{p'(r', z')} + g'z' + \frac{v'^2(r')}{2} \tag{93}$$

$$\frac{p'(r', z')}{p'_{ref}} = \left(\frac{T'_{core}(r', z')}{T'_{ref}}\right)^{\frac{\gamma}{\gamma-1}} \exp\left[-\frac{S'_{core}(r'_{min}, z'_{edge})}{R'} + \frac{L'\sigma P'[T'_{core}(r', z')]}{R'T'_{core}(r', z')p'(r', z')}\right] \tag{94}$$

C. Contour Solution

- The three equations (86), (93), and (94) are three coupled non-linear algebraic equations for $[r', z', T'_{core}(r', z')]$ where r', z' is the point on the contour where the pressure is $p'(r', z')$, an assigned value within the range $p'(r'_{min}, z'_{edge})$, $p'(r'_0, z'_{interface})$.

- This is a step-by-step progression, starting from one end point on the contour, and proceeding to the other end point on the contour. The first guess at the next point in the progression is the triplet of results holding at the last converged point.

- This is a parametric solution:

$$r'[p'], \quad z'[p'], \quad T'_{core}[p'] \tag{95}$$

  Of course, one of the other variables could have been selected as the parameter, at least in theory.

- In the bulk-vortex module

$$\frac{S'(r', z')}{R'} = ln\left(\frac{T'(r', z')}{T'_{ref}}\right)^{\frac{\gamma}{\gamma-1}} - ln\left(\frac{p'(r', z')}{p'_{ref}}\right) \tag{96}$$

The fluid particles of the core-side streamline at the contour have traversed so little distance in the boundary layer that no angular momentum has been lost, but the onset of saturation changes density, temperature, vapor mass fraction, and entropy across the contour.

VI. CORE MODULE: DERIVATION OF THE STREAMFUNCTION EQUATION (FOR A TROPICAL-STORM SCENARIO: NO EYE)

- The core model is steady, axisymmetric, inviscid, and saturated.
- So the vapor mass fraction $Y' \rightarrow Y'_s(T', p')$, with $P'(T')$ known,

$$Y'_s(T', p') = \sigma \frac{P'(T')}{p'} = 0.622 \frac{P'(T')}{p'} \tag{97}$$

  Note: Introduction of the notation Y'_s is a deviation because prime denotes dimensionality, and the vapor mass fraction is dimensionless, but the practice is a precursor that, in the saturated core, we adopt the symbol $\widetilde{Y}_s$ for the normalized vapor mass fraction.
- Y'_s is not conserved on streamlines $\eta'(r', z')$ in the core, owing to condensation.
- So there are three integrals that are constant on streamlines in the core. We present these as (98), (99), and (101).

$$E'(\eta') = c'_p T' + L' Y'_s(T', p') + g' z' + q'^2/2 \tag{98}$$

where we sometimes approximate $q'^2/2 \rightarrow v'^2/2$ but more generally $q'^2 = u'^2 + v'^2 + w'^2$.

$$S'(\eta') = c'_p ln(T'/T'_r) - R' ln(p'/p'_r) + L' Y'_s(T', p')/T' \tag{99}$$

where

$$\begin{aligned} T'_r &\equiv T'_{ref} \equiv T'(r'_0, 0) = T'_{amb}(0) \\ p'_r &\equiv p'_{ref} \equiv p'(r'_0, 0) = p'_{amb}(0) \end{aligned} \tag{100}$$

$$\Gamma'(\eta') = r' v' + \Omega' r'^2 \tag{101}$$

- $p'/p'_r = (\rho'/\rho'_r)(T'/T'_r)$

- Solving the S' equation for p'/p'_r, and substituting for $L'Y'_s$ from the E' equation give $p'\left[r', z', \eta'(r', z'), T'[r', z', \eta'(r', z')]\right]/p'_r$:

$$p'\left[r', z', \eta'(r', z'), T'[r', z', \eta'(r', z')]\right]/p'_r = \left(\frac{T'}{T'_r}\right)^{\frac{\gamma}{\gamma-1}} \exp\left[-\frac{S'(\eta')}{R'} + \frac{E'(\eta') - g'z' - q'^2/2}{R'T'} - \frac{\gamma}{\gamma-1}\right] \tag{102}$$

  Note: Equation (98) for $E'(\eta')$ is an implicit algebraic equation for $T'[r', z', \eta'(r', z')]$, once the streamfunction $\eta'(r', z')$ is found.

- Since $p' = p'[r', z', \eta'(r', z'), T'[r', z', \eta'(r', z')]]$, by the chain rule,

$$\left\{\frac{\partial p'}{\partial r'}\left[r', z', \eta'(r', z'), T'[r', z', \eta'(r', z')]\right]\right\}_{z'} = \left(\frac{\partial p'}{\partial \eta'}\right)_{T',r',z'}\left(\frac{\partial \eta'}{\partial r'}\right)_{z'} + \left(\frac{\partial p'}{\partial r'}\right)_{T',\eta',z'} + \left(\frac{\partial p'}{\partial T'}\right)_{\eta',r',z'}\left(\frac{\partial T'}{\partial \eta'}\right)_{r',z'}\left(\frac{\partial \eta'}{\partial r'}\right)_{z'} + \left(\frac{\partial p'}{\partial T'}\right)_{\eta',r',z'}\left(\frac{\partial T'}{\partial r'}\right)_{\eta',z'} \tag{103}$$

  We need this expression because we seek the streamfunction equation from the conservation of radial momentum:

$$\rho' u' \frac{\partial u'}{\partial r'} + \rho' w' \frac{\partial u'}{\partial z'} - 2\Omega'\rho' v' - \rho' \frac{v'^2}{r'} = -\left(\frac{\partial p'}{\partial r'}\right)_{z'} \tag{104}$$

  There are three partial derivatives of p' to be computed so the right-hand side of (104) is available in a useful form.

- From continuity

$$\left(\frac{\partial \eta'}{\partial r'}\right)_{z'} = \rho' w' r' \tag{105}$$

- $$c'_p T' + \frac{L'\sigma' P'(T')/p'_r}{(T'/T'_r)^{\frac{\gamma}{\gamma-1}} \exp\left\{-S'(\eta')/R' + [E'(\eta') - g'z' - q'^2/2]/(R'T') - \gamma/(\gamma-1)\right\}} = E'(\eta') - g'z' - q'^2/2 \tag{106}$$

so the following dimensionless expression is defined for convenience:

$$\Upsilon \equiv \left(\frac{T'}{T'_r}\right)^{\frac{\gamma}{\gamma-1}} \exp\left\{-\frac{S'(\eta')}{R'} + \frac{E'(\eta') - g'z' - q'^2/2}{R'T'} - \frac{\gamma}{\gamma-1}\right\} \tag{107}$$

Equation (106) is a useful form from which to obtain two needed partial derivatives of T' appearing in (103).

- From (102),

$$\left(\frac{\partial p'}{\partial r'}\right)_{T',\eta',z'} = \rho'\left[-u'\frac{\partial u'}{\partial r'} - v'\frac{\partial v'}{\partial r'} - w'\frac{\partial w'}{\partial r'}\right] \tag{108}$$

- Also from (102),

$$\left(\frac{\partial p'}{\partial \eta'}\right)_{T',r',z'} = \rho'\left[-T'\frac{dS'(\eta')}{d\eta'} + \frac{dE'(\eta')}{d\eta'} - v'\frac{\partial v'}{\partial \eta'}\right] \tag{109}$$

where we note that

$$\Gamma'(\eta') = r'v' + \Omega' r'^2 \Rightarrow v' = \frac{\Gamma'(\eta') - \Omega' r'^2}{r'} \tag{110}$$

$$\left(\frac{\partial v'}{\partial \eta'}\right)_{r',z'} = \frac{d\Gamma'(\eta')}{d\eta'}\frac{1}{r'} \tag{111}$$

Hence,

$$\left(\frac{\partial p'}{\partial \eta'}\right)_{\Gamma',r',z'} = \rho'\left[-T'\frac{dS'(\eta')}{d\eta'} + \frac{dE'(\eta')}{d\eta'} - \frac{v'}{r'}\frac{d\Gamma'(\eta')}{d\eta'}\right] \tag{112}$$

- From (106),

$$\left(\frac{\partial p'}{\partial T'}\right)_{\eta',r',z'} = \rho'\left[c'_p - \frac{E'(\eta') - g'z' - q'^2/2}{T'}\right] \tag{113}$$

- From (106),

$$\left(\frac{\partial T'}{\partial \eta'}\right)_{r',z'} = \frac{\frac{dE'(\eta')}{d\eta'}[1+\chi] - v'\left(\frac{\partial v'}{\partial \eta'}\right)_{r',z'}[1+\chi] - T'\frac{dS'(\eta')}{d\eta'}[\chi]}{c'_p + R'T'[\chi]\left\{\frac{\frac{dP'(T')}{dT'}}{P'(T')} - \frac{\gamma}{\gamma-1}\frac{1}{T'} + \frac{E'(\eta') - g'z' - q'^2/2}{R'T'^2}\right\}} \tag{114}$$

So the following dimensionless expression is defined for convenience:

$$\chi \equiv \frac{L'\sigma P'(T')/p'_r}{\Upsilon(R'T')} \tag{115}$$

- $$\left(\frac{\partial T'}{\partial r'}\right)_{\eta',z'} = \frac{-\left(u'\frac{\partial u'}{\partial r'} + v'\frac{\partial v'}{\partial r'} + w'\frac{\partial w'}{\partial r'}\right)[1+\chi]}{c_p' + R'T'[\chi]\left\{\frac{\frac{dP'(T')}{dT'}}{P'(T')} - \frac{\gamma}{\gamma-1}\frac{1}{T'} + \frac{E'(\eta')-g'z'-q'^2/2}{R'T'^2}\right\}} \tag{116}$$

  Substituting, as previously discussed, for the pressure gradient in equation (104) for conservation of radial momentum:

$$\begin{aligned}
&\rho' u' \frac{\partial u'}{\partial r'} + \rho' w' \frac{\partial u'}{\partial z'} - 2\rho'\Omega' v' - \rho' \frac{v'^2}{r'} = \\
&- \rho' \left[-T' \frac{dS'(\eta')}{d\eta'} + \frac{dE'(\eta')}{d\eta'} - v' \frac{\partial v'}{\partial \eta'}\right] \rho' w' r' \\
&- \rho' \left[-u' \frac{\partial u'}{\partial r'} - v' \frac{\partial v'}{\partial r'} - w' \frac{\partial w'}{\partial r'}\right]_{T',\eta',z'} \\
&- \rho' \left[c_p' - \frac{E'(\eta') - g'z' - q'^2/2}{T'}\right] \rho' w' r' \quad \times \\
&\left\{\frac{\frac{dE'(\eta')}{d\eta'}[1+\chi] - v'\left(\frac{\partial v'}{\partial r'}\right)_{r',z'}[1+\chi] - T'\frac{dS'(\eta')}{d\eta'}[\chi]}{c_p' + R'T'[\chi]\left\{\frac{\frac{dP'(T')}{dT'}}{P'(T')} - \frac{\gamma}{\gamma-1}\frac{1}{T'} + \frac{E'(\eta')-g'z'-q'^2/2}{R'T'^2}\right\}}\right\} \\
&+ \rho' \left[c_p' - \frac{E'(\eta') - g'z' - q'^2/2}{T'}\right] \quad \times \\
&\left\{\frac{\left(u'\frac{\partial u'}{\partial r'} + v'\frac{\partial v'}{\partial r'} + w'\frac{\partial w'}{\partial r'}\right)_{\eta',r'}[1+\chi]}{c_p' + R'T'[\chi]\left\{\frac{\frac{dP'(T')}{dT'}}{P'(T')} - \frac{\gamma}{\gamma-1}\frac{1}{T'} + \frac{E'(\eta')-g'z'-q'^2/2}{R'T'^2}\right\}}\right\}
\end{aligned} \tag{117}$$

- We take $v'(\partial v'/\partial r') \gg [u'(\partial u'/\partial r') + w'(\partial w'/\partial r')]$ in the last term

- We note:

$$-2\Omega v' - \frac{v'^2}{r'} = v'\left(\frac{\partial v'}{\partial r'}\right)_{\eta'} \tag{118}$$

$$\begin{aligned}
c_p' - \frac{E'(\eta') - g'z' - q'^2/2}{T'} &= -L'Y_s'(T')/T' \\
&= -\frac{L'}{T'}\frac{\sigma P'(T')}{p'}
\end{aligned} \tag{119}$$

- Cancel ρ' in all terms and divide each term by w':

$$\begin{aligned}
&\frac{\partial u'}{\partial z'} - \frac{\partial w'}{\partial r'} = \\
&- \rho' r' \left[-T' \frac{dS'(\eta')}{d\eta'} + \frac{dE'(\eta')}{d\eta'} - v' \frac{\partial v'}{\partial \eta'} \right] \\
&- \rho' r' \left[-\frac{L'}{T'} \frac{\sigma P'(T')}{p'} \right] \left\{ \frac{\frac{dE'(\eta')}{d\eta'} [1+\chi] - v' \left(\frac{\partial v'}{\partial r'} \right)_{r',z'} [1+\chi] - T' \frac{dS'(\eta')}{d\eta'} [\chi]}{c_p' + R'T'[\chi] \left\{ \frac{\frac{dP'(T')}{dT'}}{P'(T')} - \frac{\gamma}{\gamma-1} \frac{1}{T'} + \frac{E'(\eta') - g'z' - q'^2/2}{R'T'^2} \right\}} \right\} \\
&+ \frac{1}{w'} \left[-\frac{L'}{T'} \frac{\sigma P'(T')}{p'} \right] \left\{ \frac{\left(u' \frac{\partial u'}{\partial r'} + v' \frac{\partial v'}{\partial r'} + w' \frac{\partial w'}{\partial r'} \right)_{\eta',r'} [1+\chi]}{c_p' + R'T'[\chi] \left\{ \frac{\frac{dP'(T')}{dT'}}{P'(T')} - \frac{\gamma}{\gamma-1} \frac{1}{T'} + \frac{E'(\eta') - g'z' - q'^2/2}{R'T'^2} \right\}} \right\}
\end{aligned} \tag{120}$$

  Take $v' \frac{\partial v'}{\partial r'} \gg u' \frac{\partial u'}{\partial r'} + w' \frac{\partial w'}{\partial r'}$ in the last term.

- Since $v' = v'(\eta', r')$, a well known identity is

$$\left(\frac{\partial \eta'}{\partial r'} \right)_{v'} \left(\frac{\partial v'}{\partial \eta'} \right)_{r'} \left(\frac{\partial r'}{\partial v'} \right)_{\eta'} = -1 \tag{121}$$

  For terms in the last two lines to cancel,

$$\rho' w' r' \left(v' \frac{\partial v'}{\partial \eta'} \right) = -v' \left(\frac{\partial v'}{\partial r'} \right)_{\eta',z'} \tag{122}$$

  but $\rho' w' r' = \left(\frac{\partial \eta'}{\partial r'} \right)_{z'}$, so

$$\left(\frac{\partial \eta'}{\partial r'} \right)_{z'} \left(\frac{\partial v'}{\partial \eta'} \right)_{r',z'} \left(\frac{\partial r'}{\partial v'} \right)_{\eta',z'} = -1 \tag{123}$$

  We take this to hold to good approximation, so terms involving v' in the last two lines cancel. Therefore,

$$\begin{aligned}
&- \frac{\partial}{\partial z'} \left(\frac{1}{\rho' r'} \frac{\partial \eta'}{\partial z'} \right) - \frac{\partial}{\partial r'} \left(\frac{1}{\rho' r'} \frac{\partial \eta'}{\partial r'} \right) = \\
&- \rho' r' \left[-T' \frac{dS'(\eta')}{d\eta'} + \frac{dE'(\eta')}{d\eta'} - \frac{v'}{r'} \frac{\partial \Gamma'(\eta')}{\partial \eta'} \right] \\
&- \rho' r' \left[-\frac{L' Y_s'(T', p')}{T'} \right] \left\{ \frac{\frac{dE'(\eta')}{d\eta'} [1+\chi] - T' \frac{dS'(\eta')}{d\eta'} [\chi]}{c_p' + R'T'[\chi] \left\{ \frac{\frac{dP'(T')}{dT'}}{P'(T')} + \frac{L' Y_s'(T', p')/T'}{R'T'} \right\}} \right\}
\end{aligned} \tag{124}$$

$$Y_s'(T',p') \equiv \frac{\sigma P'(T')}{p'} \tag{125}$$

- Recall:

$$\chi \equiv \frac{L'\sigma P(T')/p_r'}{\Upsilon(R'T')} \tag{126}$$

$$\Upsilon \equiv \left(\frac{T'}{T_r'}\right)^{\frac{\gamma}{\gamma-1}} \exp\left\{-\frac{S'(\eta')}{R'} + \frac{L'Y_s'(T',p')}{R'T'}\right\} \tag{127}$$

$$\begin{aligned}
&-\frac{\partial}{\partial z'}\left(\frac{1}{\rho' r'}\frac{\partial \eta'}{\partial z'}\right) - \frac{\partial}{\partial r'}\left(\frac{1}{\rho' r'}\frac{\partial \eta'}{\partial r'}\right) = \\
&-\rho' r'\Bigg\{ -T'\frac{dS'(\eta')}{d\eta'}\left[1 - \frac{[\chi]L'Y_s'(T',p')/T'}{c_p' + R'T'[\chi]\left(\frac{\frac{dP'(T')}{dT'}}{P'(T')} + \frac{L'Y_s'(T',p')/T'}{R'T'}\right)}\right] \\
&\quad + \frac{dE'(\eta')}{d\eta'}\left[1 - \frac{[1+\chi]L'Y_s'(T',p')/T'}{c_p' + R'T'[\chi]\left(\frac{\frac{dP'(T')}{dT'}}{P'(T')} + \frac{L'Y_s'(T',p')/T'}{R'T'}\right)}\right] \\
&\quad - \frac{v'}{r'}\frac{d\Gamma'(\eta')}{d\eta'}\Bigg\}
\end{aligned} \tag{128}$$

- Nondimensionalization (ν' denotes the eddy viscosity, taken as constant, and appears in the Ekman number E and elsewhere):

$$\begin{aligned}
\widetilde{Y}_s(T,p) &\equiv Y_s'(T',p')/Y_{ref}', \qquad Y_{ref}' = Y_{amb,surface}' = Y_{amb,s}' \\
T &\equiv T'/T_{ref}' \\
p &\equiv p'/p_{ref}' \\
P(T) &\equiv P'(T')/p_{ref}'
\end{aligned} \tag{129}$$

$$\begin{aligned}
\widetilde{Y}_s(T,p) &= \frac{\sigma[P'(T')/p_{amb,s}']/(p'/p_{amb,s}')}{\sigma[(\,\mathrm{RH}\,)_{amb,s}P'(T_{amb,s}')/p_{amb,s}']/(p_{amb,s}'/p_{amb,s}')} \\
&= \frac{P(T)/p}{(\,\mathrm{RH}\,)_{amb,s}P(1)}
\end{aligned} \tag{130}$$

$$
\begin{aligned}
(\,\mathrm{RH}\,)_{amb,s} &\equiv \frac{(p'_v)_{ref}}{P'(T'_{ref})} \\
\pi_1 &\equiv \frac{L'Y'_{ref}}{c'_p T'_{ref}} \\
\Upsilon &= T^{\frac{\gamma}{\gamma-1}} \exp\left[-S(\eta) + \pi_1 \frac{\gamma}{\gamma-1}\frac{\widetilde{Y}_s(T,p)}{T}\right] \\
\chi &= \pi_1 \frac{\gamma}{\gamma-1}\frac{\widetilde{Y}_s(T,p)p}{T[\Upsilon]} \\
\pi_2 &\equiv (\Omega'^2 r'^2_o)/(c'_p T'_{ref}) \\
\pi_4 &\equiv z'^2_t/r'^2_0 \qquad (z'_t \textit{ is an alternate for } z'_{lid}) \\
S &= S'/R' \qquad (R'/c'_p) = \frac{\gamma-1}{\gamma} \\
\eta &= \eta'/\eta'_{ref} \qquad \eta'_{ref} \equiv \rho'_{ref}\Omega' r'^3_o (E/2)^{1/2} \qquad E \equiv \left(\frac{\nu'}{\Omega' r'^2_o}\right) \\
r &= r'/r'_o \qquad z = z'/z'_t \qquad p = p'/p'_{ref} \qquad T = T'/T'_{ref} \qquad \rho = \rho'/\rho'_{ref} \\
p_v &= p'_v/p'_{ref} \qquad P = P'/p'_{ref} \qquad p'_{ref} = \rho'_{ref} R' T'_{ref} \\
\Gamma &= \Gamma'/(\Omega' r'^2_o) = rv + r^2 \qquad v = v'/(\Omega' r'_o)
\end{aligned}
\tag{131}
$$

$$
\begin{aligned}
&- \frac{\partial}{\partial z}\left(\frac{1}{\rho r}\frac{\partial \eta}{\partial z}\right) - \pi_4 \frac{\partial}{\partial r}\left(\frac{1}{\rho r}\frac{\partial \eta}{\partial r}\right) = \\
-\frac{\pi_4}{\pi_2(E/2)}\Bigg\{ &- \pi_2 \frac{v}{r}\frac{d\Gamma(\eta)}{d\eta} \\
&- \frac{\gamma-1}{\gamma} T \frac{dS}{d\eta}\left[1 - \frac{[\chi]\pi_1 \widetilde{Y}_s(T,p)/T}{1+\pi_1[\widetilde{Y}_s(T,p)/T]\left(\pi_1 \frac{\widetilde{Y}_s(T,p)}{T}\frac{\gamma}{\gamma-1} + \frac{T}{P(T)}\frac{dP(T)}{dT}\right)}\right] \\
&+ \frac{dE}{d\eta}\left[1 - \frac{[1+\chi]\pi_1 \widetilde{Y}_s(T,p)/T}{1+\pi_1[\widetilde{Y}_s(T,p)/T]\left(\pi_1 \frac{\widetilde{Y}_s(T,p)}{T}\frac{\gamma}{\gamma-1} + \frac{T}{P(T)}\frac{dP(T)}{dT}\right)}\right]\Bigg\}
\end{aligned}
\tag{132}
$$

$\pi_1 \approx \mathcal{O}(0.2)$, typically

$\pi_4 \approx 10^{-3}$, $E \approx 10^{-1}$, $\pi_2 \approx 10^{-2}$, typically

VII. CORE MODULE: BOUNDARY CONDITIONS ON THE STREAMFUNCTION

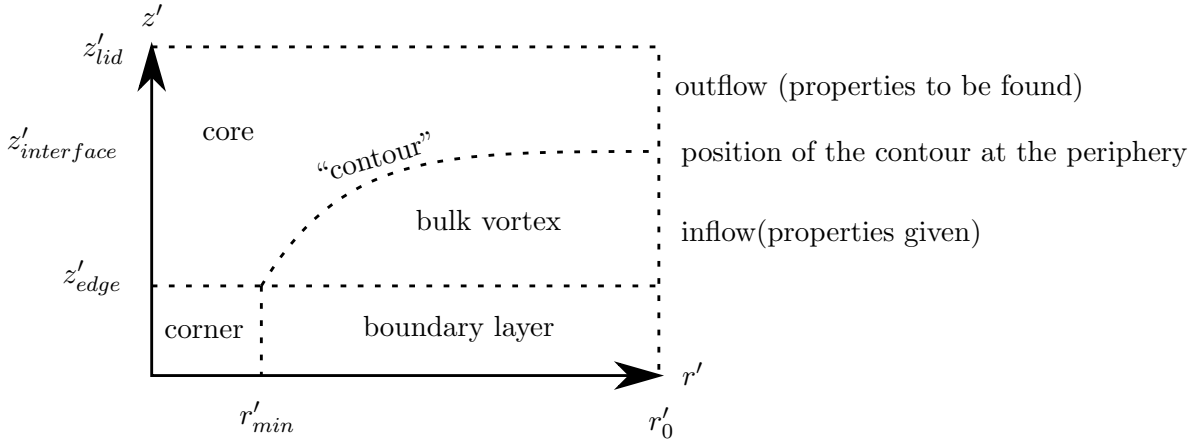

The boundary condition holding on $r' = r'_o$, $z'_{lid} \geq z' \geq z'_{interface}$ deserves discussion. We assign $\eta' = \eta_{max}$ on the contour, and $\eta' = 0$ on the central axis and lid.

$\eta'(r'_o, z')$ should decrease monotonically from $\eta' = \eta'_{max}$ at $z' = z'_{interface}$ to $\eta' = 0$ at $z' = z'_{lid}$, but we really cannot prescribe how.

$$-\rho' u'(r'_o, z') r'_o = \frac{\partial \eta'(r'_o, z')}{\partial z'} \tag{133}$$

$$-\rho' w'(r'_o, z') r'_o = \frac{\partial \eta'(r'_o, z')}{\partial r'} \tag{134}$$

$$\frac{\partial \eta'(r'_o, z')}{\partial z'} < 0 \quad \Rightarrow \quad u'(r'_o, z') > 0 \quad \text{(outflow)} \tag{135}$$

We expect $\partial \eta'(r'_o, z')/\partial r' = 0$ at $z' = z'_{interface}$ and $z' = z'_{lid}$ because these are streamlines (no crossflow), but $\partial \eta'(r'_o, z')/\partial z'$ might be discontinuous [vortex sheet: inflow below $z' = z'_{interface}$, outflow above $z' = z'_{interface}$ ... though $\partial \eta'(r'_o, z'_{interface})/\partial z' = 0$ is not excluded

(smooth transition)]. We might see whether it suffices for solution to take

$$\frac{\partial \eta'(r'_o, z')}{\partial r'} = 0 \qquad z'_{lid} > z' > z'_{interface} \tag{136}$$

The constraints holding on the entry to the core module ($z' = z_{edge}, 0 < r' < r_{min}$) are discussed below.

VIII. CORE MODULE : FINDING THE DEPENDENT VARIABLES AFTER THE STREAMFUNCTION $\eta'(r', z')$ IS IN HAND

- To have obtained $\eta'(r', z')$, we have committed to expressions for $\Gamma'(\eta')$, $S'(\eta')$, and $E'(\eta')$. So once $\eta'(r', z')$ is in hand, we may complete the solution as follows.

- $$\begin{aligned} v'(r', z') &= \left[\Gamma'(\eta'(r', z')) - \Omega' r'^2\right] / r' \\ v'(0, z') &= 0 \end{aligned} \tag{137}$$

- Simultaneous nonlinear algebraic equations for $p'(r', z')$ and $T'(r', z')$:

$$Y'_s(r', z') = \sigma P'[T'(r', z')]/p'(r', z') \tag{138}$$

$$c'_p T'(r', z') + L' Y'_s(r', z') + g' z' + \frac{v'^2(r', z')}{2} = E'(\eta'(r', z')) \tag{139}$$

$$ln\left[\frac{T'(r', z')}{T'_{ref}}\right]^{\frac{\gamma}{\gamma-1}} - ln\left[\frac{p'(r', z')}{p'_{ref}}\right] + \frac{L' Y'_s(r', z')}{R' T'(r', z')} = \frac{S'[\eta'(r', z')]}{R'} \tag{140}$$

- $$\rho'(r', z') = \frac{p'(r', z')}{R' T'(r', z')} \tag{141}$$

- $$u'(r', z') = -\frac{1}{\rho'(r', z')} \frac{1}{r'} \frac{\partial \eta'(r', z')}{\partial z'} \tag{142}$$

- $$w'(r', z') = \frac{1}{\rho'(r', z')} \frac{1}{r'} \frac{\partial \eta'(r', z')}{\partial r'} \tag{143}$$

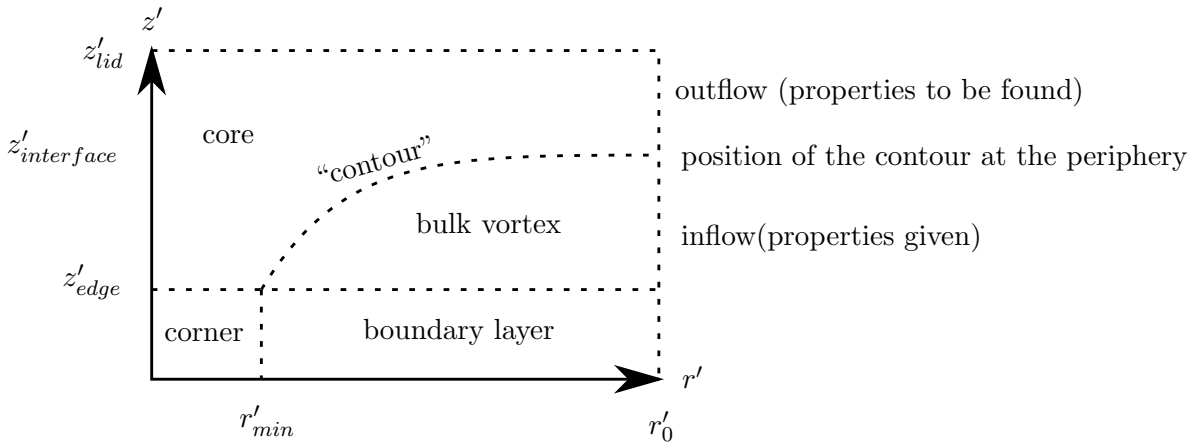

IX. NOTES ON STARTING CONDITIONS FOR THE CORE MODULE

This sketch repeated here is misleading for the saucer-like proportions of a tropical cyclone, which has diameter readily 60 times its height, though the inner portion of the core has a diameter closer to 2.5-5 times its height: $z'_{lid} \approx 12$ km while $r'_{min} \approx 30 - 60$ km and $z'_{edge} \approx 1$ km.

The Prandtl condition that $\partial p'/\partial z' \approx 0$ across the boundary-layer module (aside from hydrostatic changes) does not imply $\partial p'/\partial r' \approx 0$ across the lower core module. The average updraft in the lower core may average 100 times the downdrift speed into the boundary layer. The pressure drop from $r' = r'_{min}$ to $r' = 0$ may equal the pressure drop from $r' = r'_o$ to $r' = r'_{min}$, in the lower vortex. Short-lived core cumulonimbi may have 30-45-mph updrafts.

The case depicted is a tropical depression or tropical storm. There is no eye module, and the corner flow extends to the axis.

- We relate conditions at the exit from the corner ($0 < r' < r'_{min}, z' = z'_{edge}$) to the conditions at the entry to the corner ($r' = r'_{min}$ or $x = x_{min}$, where $x = r'^2/r'^2_o$, $0 < z' < z'_{edge}$, or $0 \leq \zeta \leq \zeta_{edge}$, where $\zeta = z'/[\nu'/(2\Omega')]^{1/2}$) We conserve mass flux (total mass/time), and distribute the total stagnation energy over streamlines at the exit from the corner as at the entry to the corner, so the total-stagnation-energy flux is

conserved.

- We do not conserve total angular momentum in the corner flow because this would imply that those fluid elements that approach closest to the axis of rotation may spin up the most. Instead, we suggest that the relative-swirl velocity component is distributed over streamlines at the exit as at the entry.

- In summary, whereas the dynamics is taken to be inviscid, and the energetics to be diffusive, in the bulk-vortex module, in contrast in the corner flow, the dynamics is taken to be dissipative, and the energetics inviscid. Saturation occurs in the corner flow. What holds along $0 < r' < r'_{min}$, $z' = z'_{edge}$, is significant because the core flow is taken to be inviscid (and saturated). Thus, to reiterate, the total angular momentum, total stagnation enthalpy, and entropy remain constant on streamlines at the value holding at entry on each streamline.

- At $z' = z'_{edge}$, $0 < r' \leq r'_{min}$,

$$\frac{\partial \eta'}{\partial r'} = \rho' w' r' \tag{144}$$

where η' is recalled to be the streamfunction. So

$$\eta'(r'_{min}, z'_{edge}) - \eta'(0, z'_{edge}) = \int_0^{r'_{min}} \rho'(r', z'_{edge}) w'(r', z'_{edge}) r' dr' \tag{145}$$

or, if $\rho'(r', z'_{edge}) w'(r', z'_{edge})$ is const,

$$\eta'_{max} - 0 = \rho'(r', z'_{edge}) w'(r', z'_{edge}) \frac{r'^2_{min}}{2} \tag{146}$$

Hence,

$$\eta'(r', z'_{edge}) = \frac{2\eta'_{max}}{r'^2_{min}} \left(\frac{r'}{2}\right)^2 \Rightarrow \frac{\eta'(r', z'_{edge})}{\eta'_{max}} = \frac{r'^2}{r'^2_{min}} \tag{147}$$

The magnitude of η'_{max} is $[\rho'_{ref} \equiv \rho'(r'_o, 0) = \rho'_{amb}(0) = \rho'_{amb,s}]$

$$\rho'_{ref} \Omega' r'^3_o (E/2)^{1/2} \int_{x_{min}}^1 \rho(x, \zeta_{edge})[-W(x)] dx \tag{148}$$

where the appearance of the Ekman Number E

$$E \equiv \nu'/(\Omega' r'^2_o) \tag{149}$$

indicates that the amount of throughput to the core related to the friction. We define

$$\eta'(r', z'_{edge}) \equiv \eta'_{edge}(r') \tag{150}$$

- We take

$$\Gamma'(r', z'_{edge}) = r'v'(r', z'_{edge}) + \Omega' r'^2 \tag{151}$$

We relate $v'(r', z'_{edge}) = v'_{edge}[\eta'_{edge}(r')]$, $\quad \eta'_{edge}(r') = \eta'_{max}(r'/r'_{min})^2$, to the swirl profile holding through the depth of the surface boundary layer at separation:

$$v'_{edge}(\eta'_{edge}(r')) = \bar{v}_{bl}\left(\eta'_{max}\frac{\eta^*}{\eta^*_{edge}}\right) = v'_{bl}(\eta^*) = \Omega' r'_o \frac{\psi[x_{min}, \zeta(\eta^*)]}{x_{min}^{1/2}} \tag{152}$$

where

$$\eta^*(x_{min}, \zeta) = -\int_0^{\zeta} \phi(x_{min}, \underline{\zeta}) d\underline{\zeta}, \qquad \psi = \frac{r'}{r'_o}\frac{v'_{bl}}{r'_o\Omega'} = r v_{bl} \tag{153}$$

$$\psi(x_{min}, \zeta) = r_{min} v(x_{min}, \zeta) = x_{min}^{1/2} v(x_{min}, \zeta) = x_{min}^{1/2} v_{bl}(\zeta) \tag{154}$$

$$\phi(x_{min}, \zeta) = r_{min} u(x_{min}, \zeta) = x_{min}^{1/2} u(x_{min}, \zeta) = x_{min}^{1/2} u_{bl}(\zeta) \tag{155}$$

where $\phi(x_{min}, \zeta)$ relates to the radial inflow in the boundary layer at separation. If $V'(r')$ denotes the (relative) swirl at the top edge of the boundary layer at radius r',

$$0 \le \eta^* \le \eta^*_{max}, \qquad 0 \le \zeta \le \zeta_{edge}, \qquad 0 \le v'_{edge} \le V'(r'_{min}) \tag{156}$$

- We take

$$E'(r', z'_{edge}) = c'_p T'(r', z'_{edge}) + L'\sigma \frac{P'[T'(r', z'_{edge})]}{p'(r', z'_{edge})} + g' z'_{edge} + \frac{V'^2}{2} \tag{157}$$

where

$$V' = \Omega' r'_o \frac{1 + \varepsilon - x_{min}}{x_{min}^{1/2}} \tag{158}$$

$$\begin{aligned} E'(r', z'_{edge}) &= E'_{edge}[\eta'_{edge}(r')] \\ &= \bar{E}'_{bl}\left(\eta'_{max}\frac{\eta^*}{\eta^*_{edge}}\right) \\ &= E'_{bl}(\eta^*) \\ &= c'_p T'_{ref} E[x_{min}, \zeta(\eta^*)] \end{aligned} \tag{159}$$

- We assign the pressure profile at the entry to the core module from the cyclostropic balance:

$$\frac{\partial p'(r', z'_{edge})}{\partial r'} = \frac{p'(r', z'_{edge})}{R'T'(r', z'_{edge})} v'^2(r', z'_{edge}) \tag{160}$$

$$p'(r'_{min}, z'_{edge}) = p'_{min} \tag{161}$$

since

$$\rho(r', z'_{edge}) = \frac{p'(r', z'_{edge})}{R'T'(r', z'_{edge})} \tag{162}$$

Cyclostrophy is integrated in conjunction with the equation for $E'(r', z'_{edge})$ to obtain $p'(r', z'_{edge})$ and $T'(r', z'_{edge})$. Density follows from the equation of state, and $w'(r', z'_{edge})$ from (146).

- We assign $S'(r', z'_{edge}) = S'_{edge}(\eta'_{edge}(r'))$ as follows:

$$\frac{S'(r', z'_{edge})}{R'} = ln\left[\frac{T'(r', z'_{edge})}{T'_{ref}}\right]^{\frac{\gamma}{\gamma-1}} - ln\left[\frac{p'(r', z'_{edge})}{p'_{ref}}\right] + \frac{L'\sigma P'[T'(r', z'_{edge})]}{R'T'(r', z'_{edge})p'(r', z'_{edge})} \tag{163}$$